Bull. Mater. Sci., Vol. 2, Number 5, December 1980, pp. 357–380. © Printed in India.

Ionic sulphate glasses*

K J RAO
Solid State and Structural Chemistry Unit, Indian Institute of Science, Bangalore 560 012, India

MS received 7 August 1980

Abstract. Sulphate glasses are typical ionic glasses in the sense they are constituted of discrete anions. In this review various physical properties of K_2SO_4, Na_2SO_4 and $ZnSO_4$ glasses have been reported. A model of random close packing of ions has been suggested and used to interpret several properties including the origin of mixed alkali effect.

Keywords. Sulphate glasses; random close packing; mixed alkali effect.

1. Introduction

Formation of glasses in purely ionic substances is comparatively less understood. The number of systems which seem to have been investigated is very few. Perhaps, the only well-investigated glasses are those of mixed nitrates. The dominant interactions in these glasses are the coulombic and the (filled shell) overlap potentials. Ionic melts generally possess low viscosities at their melting temperature and are rarely quenched into glasses from single component melts. Glasses are obtained from binary or ternary systems containing different proportions of mono and bivalent metal ions. However, small quantities of glasses can be obtained by fast quenching of pure nitrates.

A model based discussion of glasses, containing ions like nitrates, is difficult because of the geometrical complexity of such ions. Packing considerations cannot be so easily extended to them. It is in this background that we chose to investigate glasses obtained from ionic sulphate melts. Sulphate ions are tetrahedral but possess a spherical envelope of rotation. We will see later that sulphate ions lend themselves easily for building a meaningful structural model. Further sulphate glasses are much less hygroscopic than the nitrate glasses and generally have higher glass transition temperatures than the nitrate glasses. This enables many properties to be measured in glassy state over a sufficiently wide temperature range.

---

* Communication No. 78 from Solid State and Structural Chemistry Unit.

In what follows, a brief summary of the various investigations, carried out in our laboratory, has been presented. A random close-packing model is suggested and discussed which seems to be consistent with the various experimental observations.

2. Experimental investigations and results

2.1. *Phase diagram and glass formation studies*

The phase diagram of K_2SO_4–$ZnSO_4$ system was studied using differential thermal analysis. A large number of phases is indicated. The structures of all the phases are, however, not known. There are two congruently melting compounds and three eutectics. The structure of $K_2Zn_2(SO_4)_3$ corresponding to phase VI in figure 1 is known in the literature (Gattow and Zemann 1958) as cubic langbeinite. Phase IV in figure 1 that corresponds to $K_2SO_4.ZnSO_4$ is not known and we think that it may correspond to the palmierite $[K_2Pb(SO_4)_2]$ structure which is known to be rhombohedral. It may be noted that the zinc co-ordination to oxygen in $ZnSO_4$, langbeinite and rhombohedral $K_2Zn(SO_4)_2$ is uniformly six. The three eutectic and the two melting temperatures (of the two binary compounds) lie below 778 K, much below the melting temperatures of pure components.

Glasses can be easily prepared in this system by melting together $ZnSO_4.7H_2O$ and K_2SO_4, dehydrating the melt and quenching the melt by suitable methods. We found that the best method of obtaining these glasses is to quench the melt between two heavy optically polished glass slabs as shown in figure 2. By this procedure thin transparent discs about a fraction of a millimeter to 3 mm thick

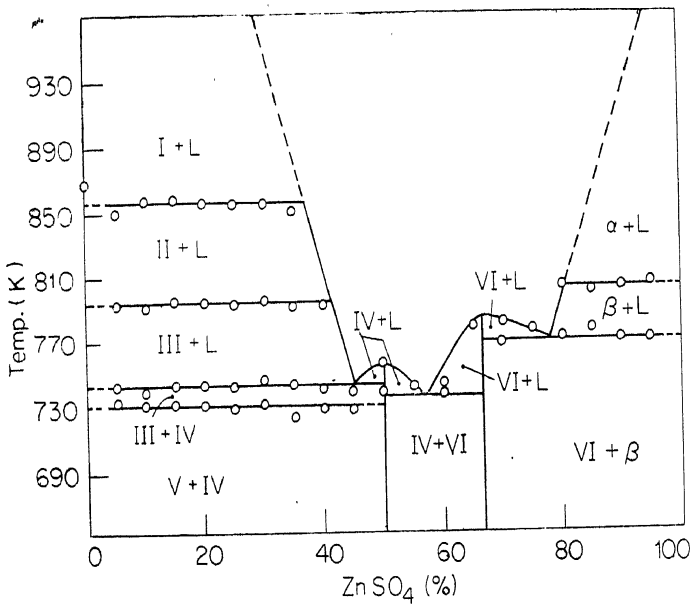

Figure 1. Phase diagram of K_2SO_4–$ZnSO_4$ system.

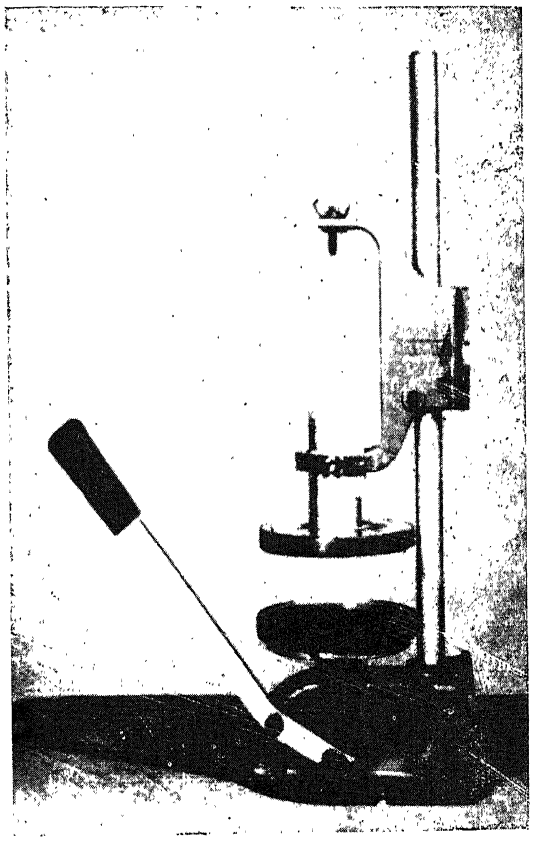

Figure 2. Quenching arrangement for making glasses.

and 3 to 5 cm in diameter are easily obtained. It is also possible to put small drops of the melt on one of the slabs and make small beads suitable for density measurements. The quenching rate attainable by this procedure has been found to be $\sim 10^2$ deg/sec. In the present studies glasses could be obtained very easily in the region 30–80% $ZnSO_4$. Zinc sulphate begins to decompose at temperatures beyond 870 K and glasses with more than 80% $ZnSO_4$ cannot be prepared. It is interesting to note the unsymmetrical nature of composition range with regard to glass formation. Phase diagram studies have not been carried out with ternary systems. But the glass formation region has been determined in K_2SO_4–Na_2SO_4–$ZnSO_4$ system and is shown in figure 3.

2.2. *Densities and molar volumes*

Densities and molar volumes of binary and ternary glasses were determined and are shown in figures 4 and 5. It may be noted that in the case of K_2SO_4–$ZnSO_4$ glasses variation of molar volume is linear indicating ideal mixing. In the ternary glasses the graph indicates the effect of intersubstitution of alkalies. The density change on crystallization in several cases is as high as 6–8% as indicated in figure 4. Further, in binary sulphates glass molar volumes can be extrapolated to the pure (hypothetical) K_2SO_4 glass and this volume corresponds to what one would expect from an extrapolation of K_2SO_4 melt volumes on a volume-temperature plot.

2.3. *Refractive indices and molar polarizations*

The refractive indices and molar polarizations of binary glasses are shown in figure 6. Here again it may be noted that the molar refraction varies linearly

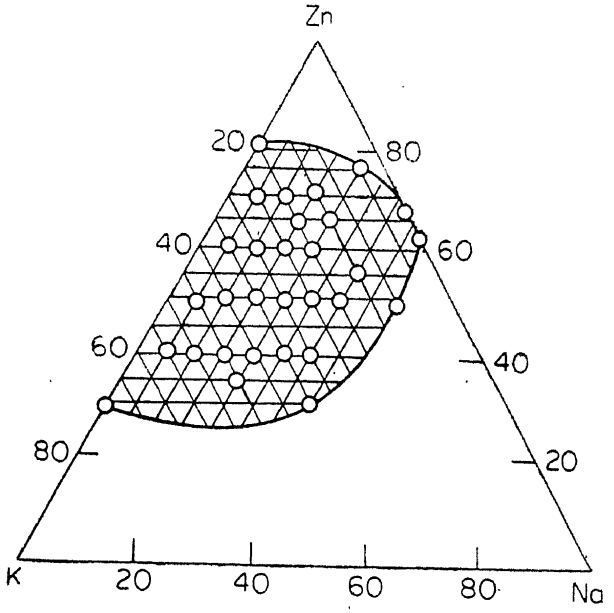

Figure 3. Glass forming region in the ternary K_2SO_4–Na_2SO_4–$ZnSO_4$ system.

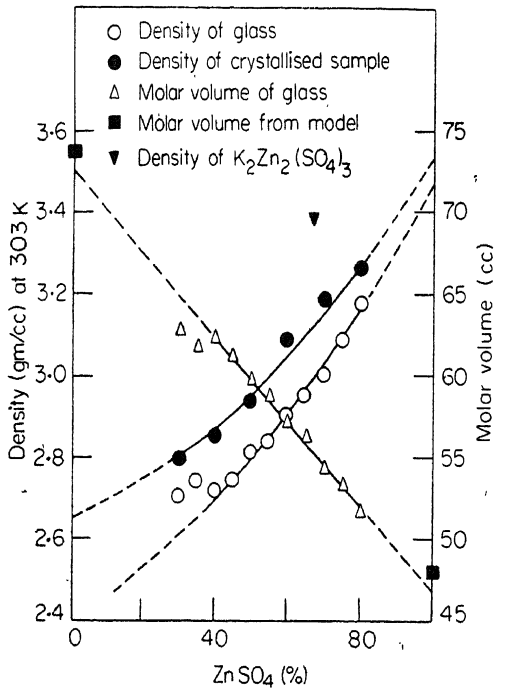

Figure 4. Densities and molar volumes of K_2SO_4–$ZnSO_4$ glasses.

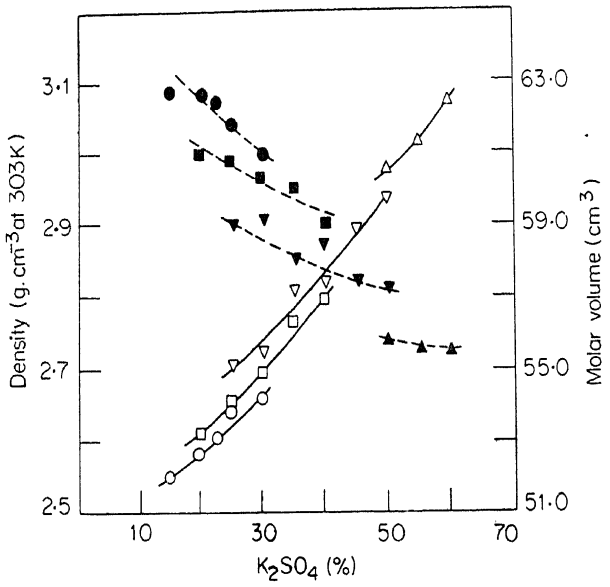

Figure 5. Densities and molar volumes of ternary glasses. Filled symbols represent densities and the open symbols correspond to molar volumes. The fixed percentages of $ZnSO_4$ corresponding to various symbols are ●, ○: 70 ; ■, □ : 60; ▼, ▽ : 50; ▲, △ : 40.

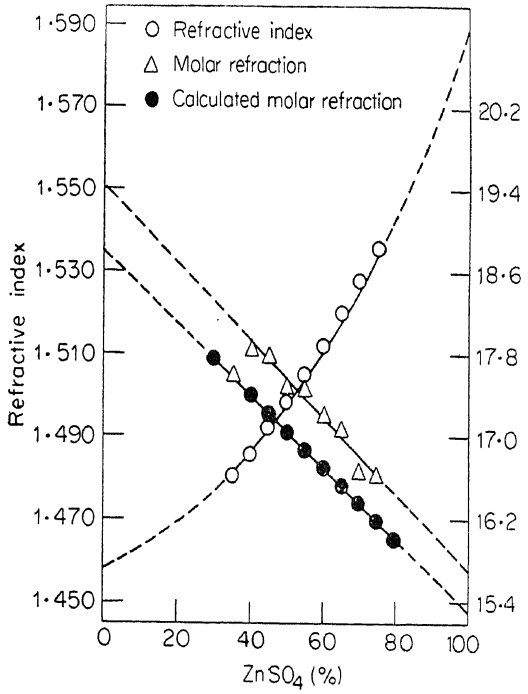

Figure 6. Refractive indices and molar refraction for binary glasses.

and is equal to the sum of ionic polarizations except for a systematic error (which could be due to the error in the reported ionic polarizations). This is reflected in the case of ternary glasses also. Together, molar volume and molar refractivity variations indicate sufficiently well that the ionic nature of bonding is fully preserved in these glasses.

2·4. *Microhardnesses and elastic constants*

Vicker microhardness measurements were carried out for binary and some ternary glasses. Generally their values lie between 100–200 kg/mm^2. Measurements on binary glasses are given in table 1. It will be shown later that these values are consistent with those obtained from the equation of Yamane and Mackenzie (1974). Elastic constants were determined using ultrasonic pulse echo technique at 10 MHz frequency. The Lame constants, bulk moduli and other relevant elastic data on K_2SO_4–$ZnSO_4$ glasses are given in table 2.

2·5. *Thermal measurements*

Glass transition and crystallization studies of binary glasses were performed using simple DTA. Several of these studies were repeated on a differential scanning calorimeter (Perkin Elmer DSC–2). Heat capacity measurements of ternary glasses were also performed using differential scanning calorimeter. The glass transition

Table 1. Microhardnesses of sulphate glasses.

Percentage of $ZnSO_4$ in glasses	Observed microhardness in kg/mm^2	Calculated microhardness in kg/mm^2
35	202·6	..
40	171·4	123·32
45	150·7	115·38
50	158·5	151·01
55	127·5	181·41
60	107·4	165·08
65	130·4	145·51
70	180·1	..

Table 2. Plastic properties of $K_2SO_4 - ZnSO_4$ glasses.

Percentage of $ZnSO_4$ in glass	Longitudinal velocity ($\times 10^5$ cm/s)	Shear velocity ($\times 10^5$ cm/s)	Lame's first constant ($\times 10^{10}$ dyn/cm^2)	Lame's second constant (10^{10} dyn/cm^2)	Young's modulus (10^{10} dyn/cm^2)	Bulk modulus (10^{10} dyn/cm^2)	Poisson's ratio
40	2·0389	0·8580	7·27	1·99	5·56	8·60	0·39
45	2·1243	0·7050	9·66	1·36	3·93	10·57	0·43
55	2·621	0·8280	15·64	1·95	5·63	16·94	0·44
65	2·0816	0·8065	8·95	1·92	5·42	10·24	0·41

temperature (T_g) and the crystallization temperature (T_{cr}) for the binary glasses are shown in figure 7. The ratios T_g/T_l, where T_l is the liquidus temperature (known from the phase diagram studies) are also shown in figure 7. It may be noted that the ratio, T_g/T_l, is roughly 2/3 for these glasses. The variation of glass transition temperatures is not related in any simple manner to percentage of $ZnSO_4$, although such simple variation has been observed in the case of nitrate glasses (Rao *et al* 1973; Angell and Helphrey 1971). In figure 8 variation of glass transition temperatures in the ternary K_2SO_4–Na_2SO_4–$ZnSO_4$ glasses are presented as a function of inter-alkali variation. It is interesting to note that the T_g increases with the increase in K_2SO_4. If any of the low energy vibrational frequencies associated with the alkali ion are directly related (Miller 1979) to glass transition temperature we should have observed just the opposite trend of variation in T_g.

The measured heat capacities of various ternary glasses are presented in figure 9.

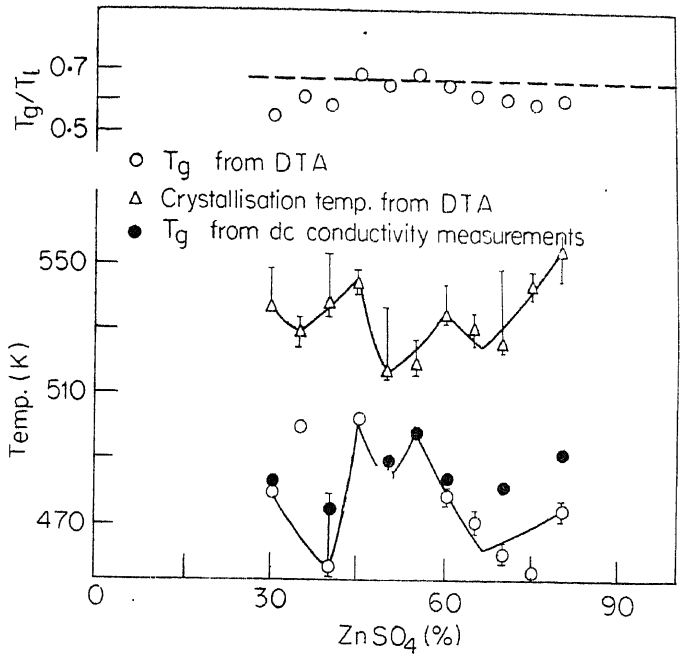

Figure 7. Glass transition and crystallization temperatures of binary sulphate glasses.

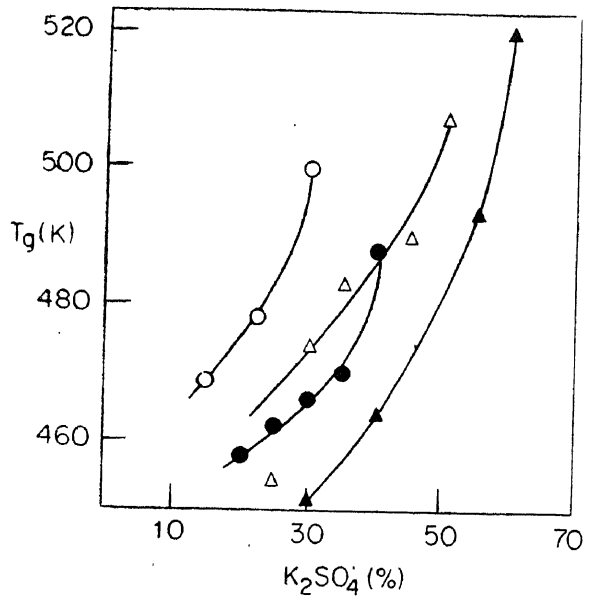

Figure 8. Glass transition temperatures of ternary glasses. The symbols ○, ●, △ and ▲ corresponds to fixed 70, 60, 50 and 40% $ZnSO_4$ in the glass. The percentage of K_2SO_4 in the glass is indicated on the x-axis.

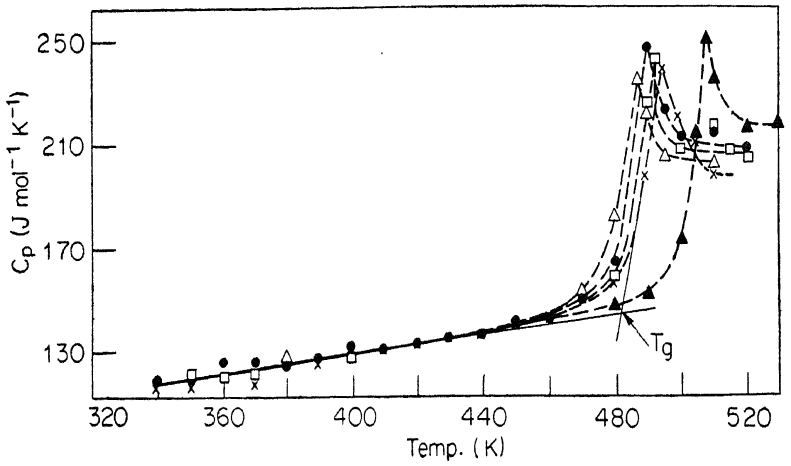

Figure 9. Heat capacities of ternary glasses containing 70 $ZnSO_4$ as a function of temperature. The symbols ▲, ×, □, ● and △ correspond to 30, 25, 22·5, 20 and 15% K_2SO_4 and remaining Na_2SO_4 in the glass.

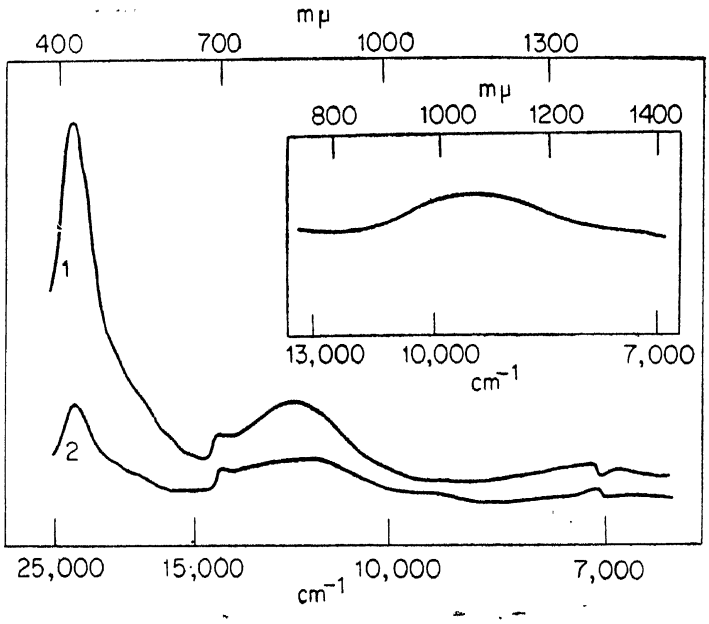

Figure 10. Spectra of Ni^{2+} doped glasses. Spectra of Fe^{2+} doped glass (inset).

2.6. *Probe ion spectroscopy*

The site symmetries of ions in glasses are often easily determined by doping with transition metal ions and studying their optical spectra. The sulphate glasses in our studies were doped with transition metal ions, Fe^{3+}, Fe^{2+}, Co^{2+}, Ni^{2+} and Cu^{2+}, (the electronic structure of the ions correspond to d^5–d^9). Dopant concentrations were kept at less than 1% and the spectra were recorded in the region 400–1500 nm. The spectra of Co^{2+}, Ni^{2+} are given in figures 10 and 11. The

spectra of Fe^{2+} is given in the inset of figure 10. Fe^{3+} did not give good spectra while Cu^{2+} gave a broad absorption around 11200 cm^{-1}. The absorption peaks exhibit no significant shifts and are very similar over the entire range of glass compositions. The absorption frequencies, their assignments and other spectral paramaters are listed in tables 3 and 4. The Racah parameters of Ni^{2+} and

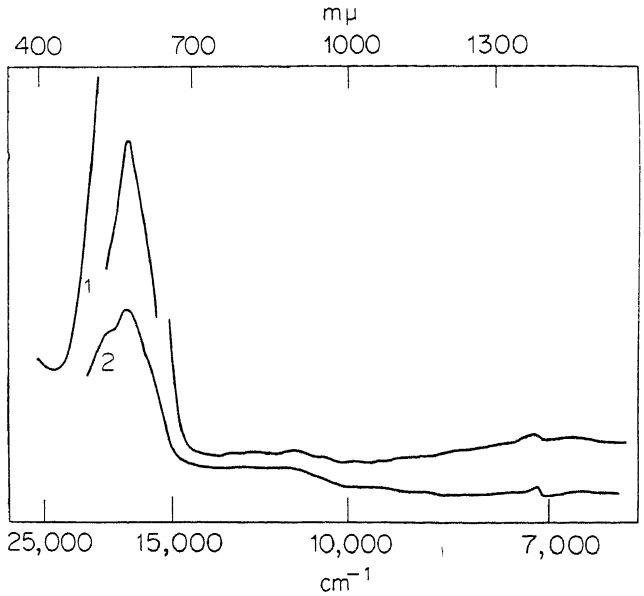

Figure 11. Spectra of Co^{2+} in (1) 70 : 30 and (2) 20 : 80 K_2SO_4 : $ZnSO_4$ glasses.

Table 3. Absorption maxima in cm^{-1} from the spectra.

Dopant ion* \ Glass composition K_2SO_4 : ZnSO	70 : 30	60 : 40	50 : 50	35 : 65	20 : 80
Fe^{2+}	..	..	..	9300 wb	..
Co^{2+}	6890 wb (15·1)	..	..	..	6870 vw (39·5)
	11100 wb (13·4)	11900 wb	..	..	11040 vw (44·6)
	17360 vs (73·7)	17240 s	17240 s	..	17360 s (82·3)
	18450 sh	18380 sh	18690 sh	..	18690 sh
Ni^{2+}	6910 vw (12·1)	7350 vwb	7140 vw	..	6800 vw (20·2)
	12050 s (19·4)	11980 wb	12120 b	..	11700 wb (26·6)
	14160 w (16·2)	14140 w	14920 s	..	14290 w (24·3)
	22520 vs (48·3)	22220 s	22220 vs	..	22730 s (37·6)
Cu^{2+}	11270 b (71·2)	11630 b	11630 b	..	11150 b (48·9)

* The concentrations of the dopant ion in the (70 : 30) and (20 : 80) compositions were 0·3 and 0·39 moles/litre respectively and the dopant ion concentrations in all other glasses ar approximately 0·2 moles/litre.

s : strong, w : weak, b : broad, sh : shoulder, vs : very strong, vw : very weak, wb : weak and broad.

Table 4. Assignment of transitions and the transition energy parameters.

Dopant ion	Observed transition cm^{-1}	Assignment	Calculated transition cm^{-1}	Ligand field splitting energy cm^{-1}	Racah parameter cm^{-1}
Fe^{2+}	9300	$^5\Gamma_5$ (D) → $^5\Gamma_3$ (D)	9300	9300	..
Co^{2+}	6870	$^4\Gamma_4$ (F) → $^4\Gamma_5$ (F)	6870	7490	720
	11040	→ $^4\Gamma_2$ (F)	13880	..	
	17360	→ $^4\Gamma_4$ (P)	16360	..	
Ni^{2+}	6800	$^2\Gamma_2$ (F) → $^3\Gamma_5$ (F)	6880	6860	880
	11700	→ $^3\Gamma_4$ (F)	11450	..	
	14290	→ $^1\Gamma_3$ (D)	14910	..	
	22730	→ $^3\Gamma_4$ (P)	22360	..	
Cu^{2+}	11150	$^2\Gamma_3$ (D) → $^2\Gamma_5$ (D)	11200	11200	

Co^{2+} ions are found to be fairly close to the free ion values (Bates 1960) (Co^{2+} 971 cm^{-1}; Ni^{2+} 880 cm^{-1}). These spectral features indicate clearly that zinc ions (whose positions are taken up by the dopant transition metal ions) are always present in octahedral environment over the entire range of glass compositions.

2.7. *Dielectric properties*

Dielectric permittivities and losses of binary sulphate glasses have been investigated as a function of temperature at 1 kHz (Narasimham *et al* 1979a). The behaviour of the loss (tan δ) as a function of temperature is shown in figure 12 for various compositions. It is clear in all these cases that the loss peak appears 25–30° below the glass transition temperatures. In the case of 30 : 70 and 60 : 40 (K_2SO_4 : $ZnSO_4$) glasses, however, small loss peaks appear at still lower temperatures. Annealing did not seem to produce significant changes except slight shifting of the dielectric loss peaks as shown in figure 13. The real part of the dielectric constant also exhibited a steep rise around the glass transition temperature. The presence of such sub-glassy loss (referred to as β-relaxation peaks) supports the view that β-peaks are perhaps a universal feature of the glassy state (Johari and Goldstein 1970). The rapid rise in the dielectric constant is more probably due to (a) contribution from both dipolar polarization and electrode polarization terms or (b) due to enhancement of complex part of conductivity rather than softening (Glass *et al* 1977) of 'soft local units'. It is unlikely that it represents ferroelectric behaviour in these glasses.

2.8. *Electrical conductivities*

DC electrical conductivities of both binary and ternary glasses have been studied as a function of temperature (Narasimham *et al* 1979b; Rao and Sundar 1980). Arrhenius plots of electrical conductivities of binary K_2SO_4–$ZnSO_4$ glasses are given in figure 14. The conductivity plots generally exhibit three linear regions

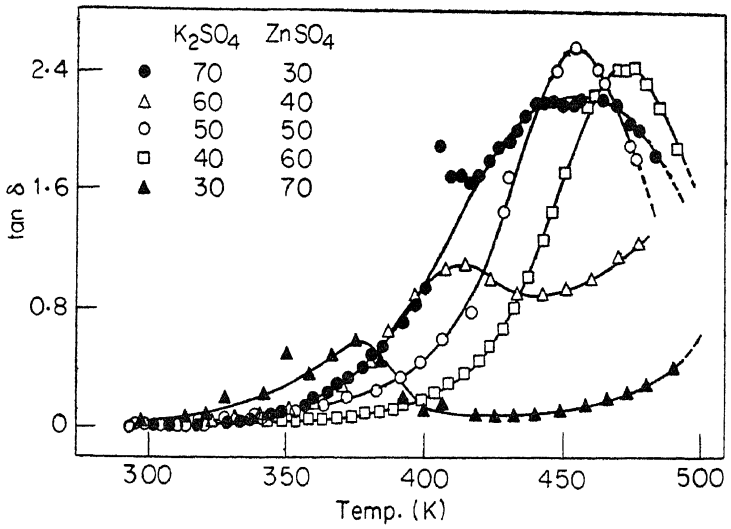

Figure 12. Behaviour of dielectric loss ($\tan\delta$) as a function of temperature in various binary glasses.

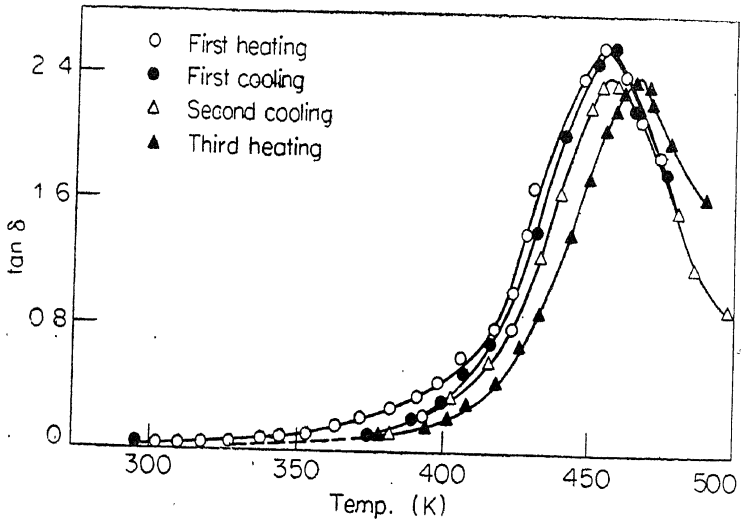

Figure 13. Effect of annealing on the dielectric loss behaviour.

and the high temperature change of slope occurs at T_g. The isothermal conductivities in all the three regions exhibit maxima around 50% $ZnSO_4$ as shown in figure 15. The activation energies for the three regions are shown in figure 16 as a function of composition and also as a function of density (in inset). It is interesting to note that the activation energies for the two subglassy regions remain essentially constant over the entire composition range, while the activation energies for the post-glass transition region increase as a function of concentration of $ZnSO_4$. It will be seen later that these findings are in agreement with the structural features of these glasses. The Arrhenius plots for the conductivities of ternary glasses are given in figure 17. It may be noted that the three-region

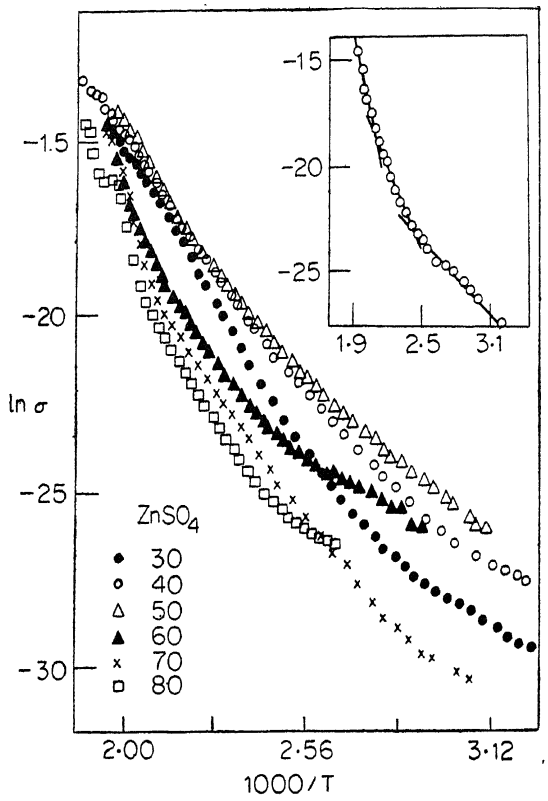

Figure 14. Arrhenius plots of d.c. conductivities of K_2SO_4–$ZnSO_4$ glasses. Inset corresponds to 60 : 40 glass and delineation of three linear regions.

feature is not observed in ternary glasses and we generally see only one subglassy activation energy. In figure 18, variation of log σ as a function of the fraction of one of the alkalies is given for three sets of glasses, each with a separate but constant fraction of $ZnSO_4$. These standard plots confirm the occurrence of mixed alkali effect in ionic glasses. The behaviour of activation energies, and log σ_0 are also shown in figures 19 and 20 respectively. Here again the occurrence of maxima confirms the phenomenon of mixed alkali effect. To our knowledge it is the first clear evidence of mixed-alkali effect in ionic glasses. We will discuss later how the origin of this effect can be attributed to the presence of microscopic strain fields inherent in the structure of these glasses.

We can use some of the results summarized above to develop a model for these glasses. Two such important results are (i) the ideal mixing in the binary K_2SO_4–$ZnSO_4$ as evidenced by molar volumes and (ii) the unaffected ionicity of the constituent ions as revealed by molar polarizations. Another important feature is the constancy of octahedral environment of zinc ions in the entire composition range. Further, if one considers the ionic potentials F_i of the cations in these glasses the increase in ionic potential $\triangle F_i$ varies with decrease in volume $\triangle V$ as shown in figure 21. Based on these features, the following model has been developed for the sulphate glasses.

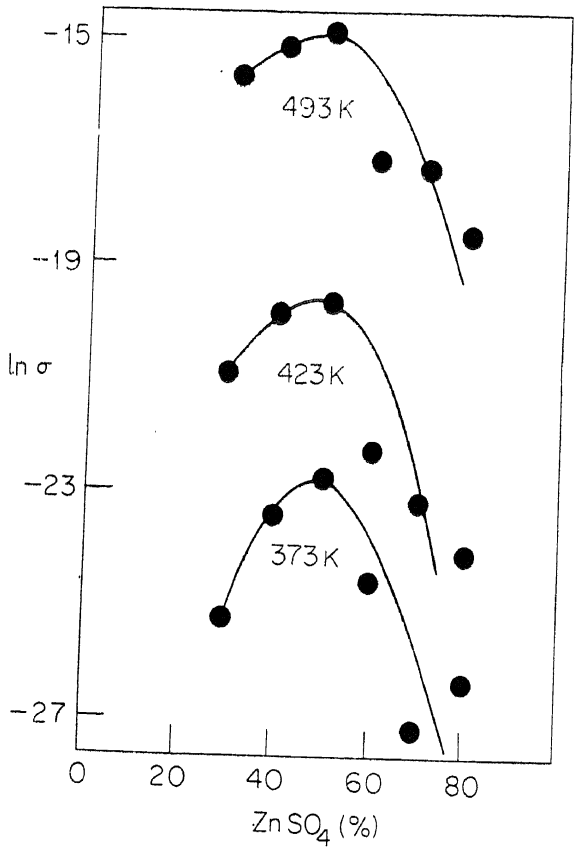

Figure 15. Isothermal conductivities of sulphate glasses.

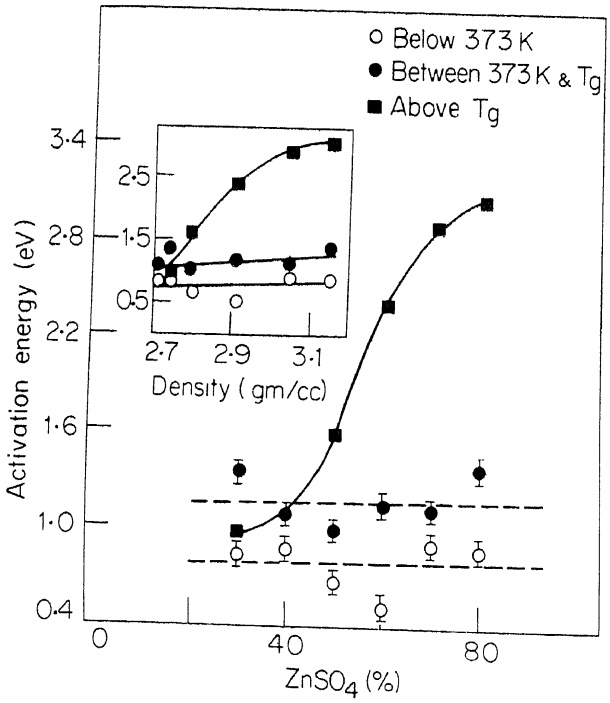

Figure 16. Activation energies in various temperature ranges of sulphate glasses as a function of composition. Inset shows the same variation as a function of density

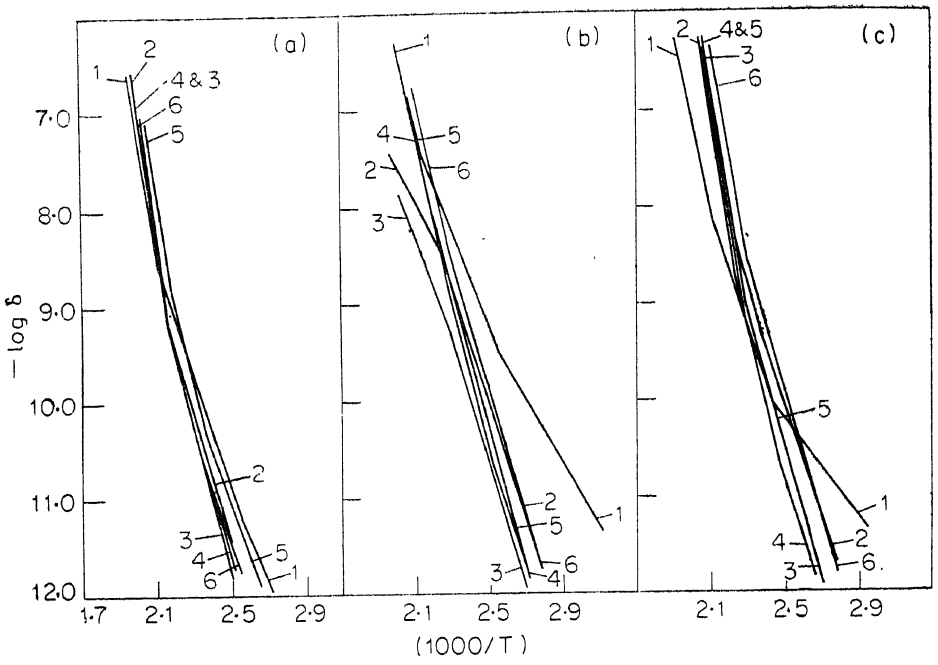

Figure 17. Arrhenius plots of d.c. conductivities of ternary glasses. $ZnSO_4$ concentration for (a), (b) and (c) are 70, 60 and 50% respectively with inter alkali variations.

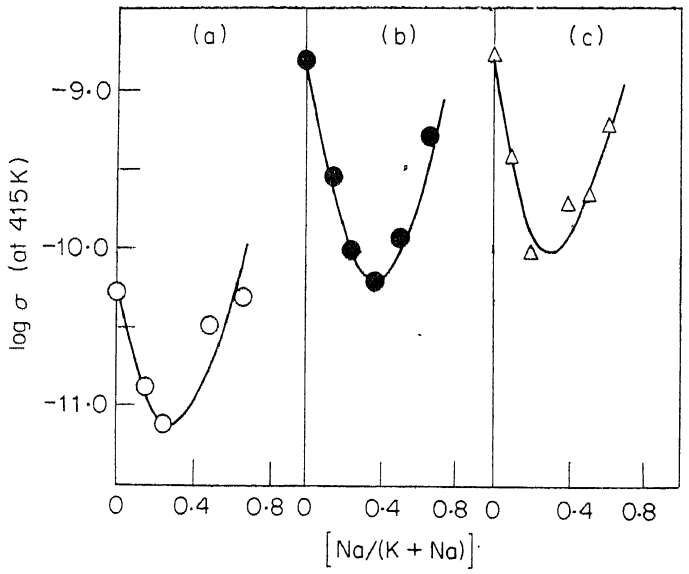

Figure 18. Conductivity variation at 415 K due to mixed-alkali effect. (a), (b) and (c) correspond to 70, 60 and 50% $ZnSO_4$ respectively.

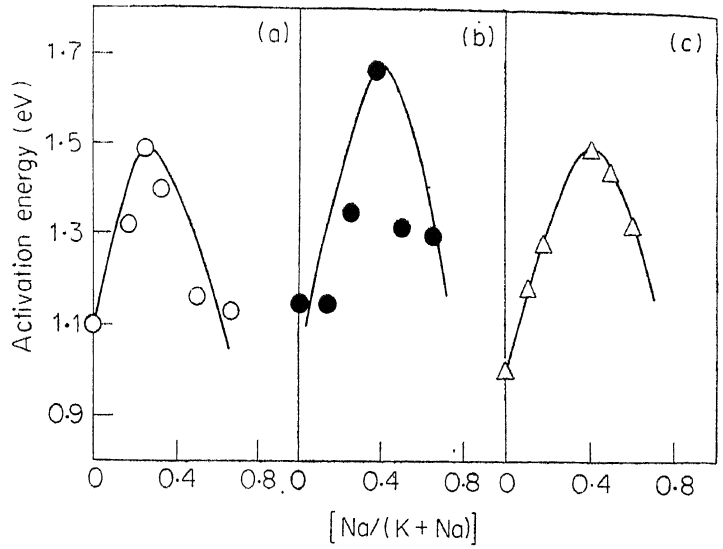

Figure 19. Mixed-alkali effect in ternary glasses (activation energies). (a), (b) and (c) have same proportions of $ZnSO_4$ as in figure 18.

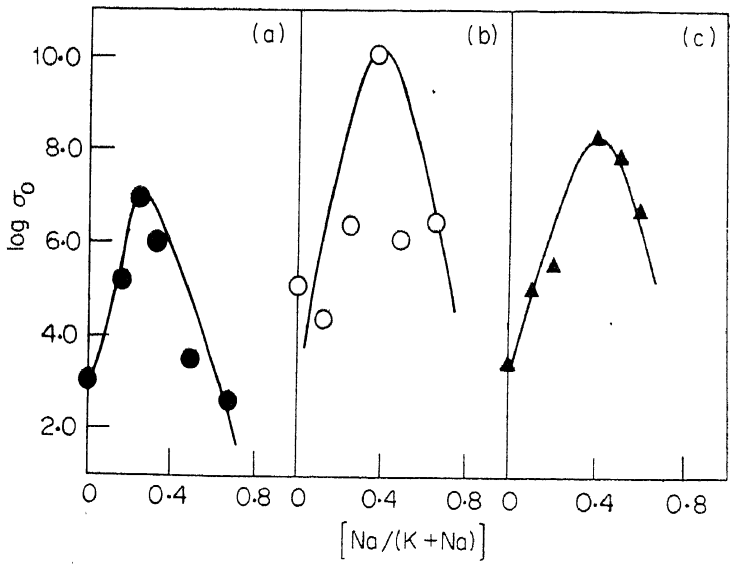

Figure 20. Mixed-alkali effect in ternary glasses (log σ_0). (a), (b) and (c) have proportions of $ZnSO_4$ as in figure 18.

3. The random close-packing model

As pointed out earlier, sulphate ions have a spherical envelope of rotation. We consider these ions for the purpose of the model, as spherical and we assume that these 'spherical' ions are random close packed (Narasimham and Rao 1978a ; Sunder and Rao 1980). The cations are assumed to be inserted into

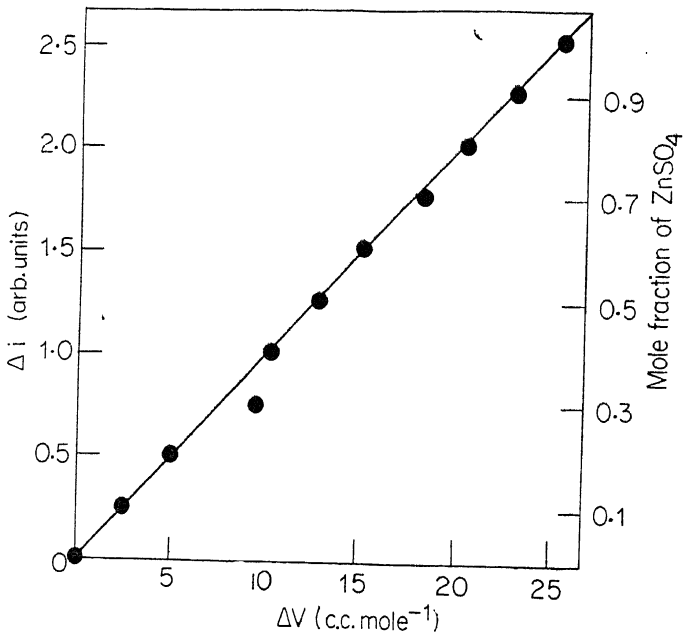

Figure 21. Variation of $\triangle F_i$ with $\triangle V$ (see text) in binary sulphate glasses.

voids in the close packed structure. The configurations around cations get modified suitably and this modified structure is revealed in the experimental observations.

The random close packing (Bernal 1965 ; Polk 1970 ; Cargill 1975) of spheres gives rise to a packing efficiency of 0·64 for the dense and 0·60 for the loose random close packing respectively. (The radius of the sulphate ion sphere is equal to 2·65 A and those of K^+, Zn^{2+}, O^{2-} are 1·33, 0·74, 1·32 A, respectively). Further, random close packing generates mostly tetrahedral voids. When one mole of sulphate ions are random close packed, almost three moles of tetrahedral voids are generated. The four sulphate spheres around tetrahedral voids may be tilted as shown in figure 22, so that a K^+ ion fits in snugly into the tetrahedral hole making contact with twelve oxygen (three each of which are provided by the four surrounding sulphate ions). In this process the net volume is not altered. But when Zn^{2+} ions are put into these tetrahedral holes, due to their high field strengths they pull the sulphate ions closer to themselves. In the extreme case (hypothetical $ZnSO_4$ glass) where only zinc ions are present we assume that the tightly packed sulphate ions are completely interlocked. Further, in order to be consistent with the spectroscopic observations, we assume that Zn^{2+} ions modify their environment and achieve octahedral co-ordination.

We can calculate the molar volume of the glasses on the basis of this model as follows. In the extreme hypothetical K_2SO_4 glass the molar volume should correspond to the random close-packing volume of one mole of 'spherical' sulphate ions which is equal to

$$(4\pi/3)\ (2\cdot65)^3\ 10^{-24} \cdot \frac{N}{0\cdot637} = 73\cdot7 \text{ cc.}$$

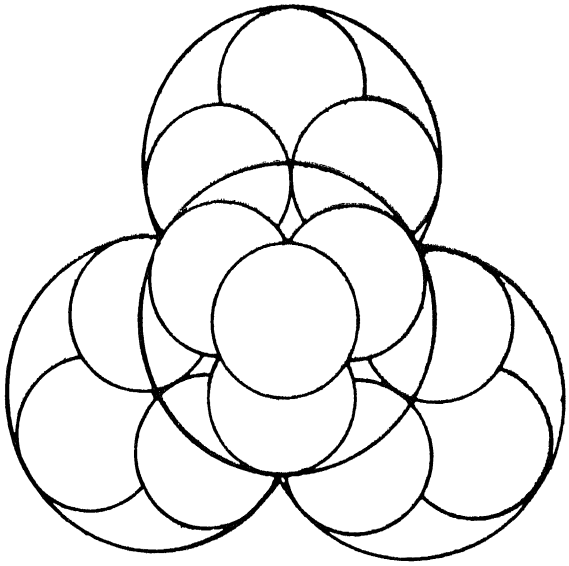

Figure 22. Model of sulphate ions 'spheres' surrounding a potassium ion. The potassium ion itself, however, is eclipsed by the oxygens.

This is indicated in figure 4 and is very close to 72·5 cc obtained from extrapolation of experimental values. For the case of pure $ZnSO_4$ glass (hypothetical) the molar volume is calculated as follows. The sulphate ions are first packed in a completly interlocked manner which roughly corresponds to a random close packed arrangement of $4N$ oxygen ions. Into one of the smaller resulting tetrahedral holes Zn^{2+} ion is pushed in. As a result the four surrounding sulphates move apart and the net volume is increased. Two more sulphates are shuffled into this assembly giving an octahedral co-ordination to Zn^{2+} ion and we assume that this latter process will not involve any change in volume. The random close packing of $4N$ oxygen ions corresponds to 38·7 cc if we take the oxygen ion radius as 1·32 A. The radius of the tetrahedral hole formed by oxygen ions is equal to $0{\cdot}225 \times 1{\cdot}32 = 0{\cdot}297$ A. When the zinc ion is forced into such a hole the radius of the hole is increased by 0·443 A. The initial 'effective radius' of a group of four sulphate ions is equal to $(3V_4/4)^{1/3}$ where V_4 is equal to $(38{\cdot}7 \times 16/4N)$ cc. When the sulphate ions are moved outwards, the net increase in volume, $\triangle V$, is equal to

$$\triangle V = \frac{4\pi}{3}\left[(r_{eff} + 0{\cdot}493)^3 - r_{eff}^3\right].$$

In the next stage of 'shuffling in' of two more sulphate ions we assume that there is no volume change. The change in volume per sulphate ion may be considered as $(\triangle V/6)$. Hence, the volume of hypothetical $ZnSO_4$ glass is $38{\cdot}7 + N\triangle V/6$ which is equal to 48.4 cc. This value is also shown in figure 4, and is in satisfactory agreement with the extrapolated experimental value (47·0 cc). Since we assume that zinc and potassium ions acquire their own characteristic environment, the molar volumes of various compositions vary linearly between these extremes.

The co-ordination numbers of zinc and potassium ions in the glasses are 6 and 4 respectively in this model. We can therefore estimate the average bond energy in the glass as (total cohesive energy)/[2 $(1-f)$. $4+f.6)$], where f is the mole fraction of $ZnSO_4$. Using this approximate value of average bond energy, a, and $C \simeq 0{\cdot}36$ the microhardness may be calculated using the formula (Yamane and Mckenzie 1974) $H_v = C(aGK)^{1/2}$ where G and K are shear and bulk modulii respectively. The calculated values were found to be satisfactory (table 1).

Dielectric loss behaviour observed in the binary glasses, we believe, are due to the jumps exhibited by K^+ ions into the neighbouring voids.

Since Zn^{2+} and K^+ ions maintain the same kind of primary co-ordination, activation barriers for their migration also remain essentially the same as observed experimentally. Sigmoidal increase of activation energy in the post-glass transition region is probably due to formation of ionic clusters around Zn^{2+} ions which migrate as heavy charged entities. The occurrence of conductivity maxima can also be explained assuming the total conductivity σ to be equal to $\sigma_{K^+} + \sigma_{Zn^{2+}}$. Contribution of zinc ions to conductivity is likely to depend upon the existence of the larger tetrahedral voids since it has to have a sufficiently large void to jump into. Hence

$$\sigma = \sigma_{K^+} + \sigma_{Zn^{2+}},$$

$$= 2(1-x)A_1 \exp(-E_1/RT) + xC_tA_2 \exp(-E_2/RT),$$

where x is the mole fraction of $ZnSO_4$ and C_t the concentration of tetrahedral voids and E_1 and E_2 are the activation barriers for K^+ and Zn^{2+} ions. The concentration C_t of tetrahedral voids can be taken as equal to $(1-x)$ moles. Therefore the total conductivity σ may now be written as

$$\sigma = B_1(1-x) + B_2x(1-x),$$

where $B_1 = 2A_1 \exp(-E_1/RT)$,

and $B_2 = A_2 \exp(-E_2/RT)$.

By equating $(\partial\sigma/\partial x)$ to zero we except a maximum in conductivity at $x = (B_2 - B_1)/2B_2$. B_1 is generally much less than B_2 so that x is approximately equal to $0{\cdot}5$ (B_1 and B_2 can be determined from experimental data at two different temperatures) as shown in figure 15.

The conductivity behaviour of ternary glasses can also be understood from this model. Na^+ ions occupy the same tetrahedral voids as K^+ ions do. In the case of Na^+ ion the sulphate ions tilt in a manner that any two oxygens of each tetrahedra approach sodium ions slightly collapse on to it thereby producing a primitive cube of oxygen ions around Na^+ ion. Here again the radius ratio of $Na^+ : O_2^{2-} :: 0{\cdot}97 : 1{\cdot}32$ which is $= 0{\cdot}73$ is ideal for body centred co-ordination from packing considerations. When the tetrahedra collapse slightly in this manner, it produces elastic strains and some amount of interlocking. Both these effects tend to immobilize the K^+ ions in the immediate surroundings. Additionally the strains enhance the activation barrier as long as strain fields do not overlap and effect a cancellation (as in dislocations). We assume that the activa-

tion energy $\triangle E$ is dependent on the concentrations of both Na^+ and K^+ ions and hence is of the form

$$\triangle E = E_0 [2(1-x)f][2(1-x)(1-f)]$$
$$= 4E_0(1-x)^2 f(1-f),$$

where E_0 is a constant in units of energy, x and f are mole fractions of Zn^{2+} and Na^+ ions respectively. The two terms in the square bracket represent concentration of Na^+ and K^+ ions respectively. Hence, it is possible to write the total conductivity σ_t as

$$\sigma_t = 2(1-x)f \cdot A_{Na^+} \cdot \exp\left\{\frac{(-E_{Na^+} - 4E_0)(1-x)^2 f(1-f)}{RT}\right\}$$
$$+ 2(1-x)(1-f) A_{K^+} \cdot \exp\left\{\frac{-E_{K^+} - 4E_0(1-x)^2 f(1-f)}{RT}\right\}$$
$$+ x \cdot A_{Zn^{2+}} \cdot \exp\left\{\frac{-E_{Zn^{2+}}}{RT}\right\}$$
$$- 4(1-x)^2 f(1-f) A_{K^+} \cdot \exp\left\{\frac{-E_{K^+}}{RT}\right\}.$$

In the above expression, we can make a simplifying assumption that the pre-exponential factors, A_{Na^+} and A_{K^+} are related to each other as

$$\left(\frac{A_{Na^+}}{A_{K^+}}\right) = \left(\frac{M_{K^+}}{M_{Na^+}}\right) = 1/\mu$$

where μ is reduced mass. Further, experimentally it is evident that there is only one activation energy in the sub-glassy region which may be interpreted as a common energy barrier experienced by the alkali ions, so that $E_{Na^+} = E_{K^+}$. Therefore,

$$\sigma_t = B_1 f \exp\left\{\frac{-4E_0 f(1-x)^2(1-f)}{RT}\right\}$$
$$+ B_1 \cdot (1-f) \exp\left\{\frac{-4E_0 f(1-x)^2(1-f)}{RT}\right\} + B_3$$
$$- 2(1-x) f(1-f)\mu B_1,$$

where B_1 and B_3 have been written for

$$2(1-x) A_{Na^+} \exp[-E_{Na^+}/RT] \text{ and } x A_{Zn^{2+}} \exp[-E_{Zn^{2+}}/RT]$$

respectively.

Here again we seek to find out the values of f for which σ_t exhibits maxima. Upon differentiation with respect to f at constant x and on rearranging the terms we can write

$$(1-2f) = \exp\left\{\frac{-4E_0(1-x)^2(1-f)f}{RT}\right\}$$
$$\times \left\{\frac{1-\mu}{2\mu(1-x)} - \frac{4E_0(1-x)[f+\mu(1-f)][1-2f]}{2RT\mu}\right\}.$$

The value of f which satisfies the equation was found by a graphical method (by plotting both sides of the expression as a function of f) and the solutions are shown in figure 23. The values indicated by arrows lie between 0·35 and 0·45 (as compared to experimental values of 0·3 to 0·4) for an assumed E_0 values of 1 kcal. The merit of the above equation for σ_t is that it involves both the size effect which is reflected in $\triangle E$ and the mass effect through μ in the pre-exponential factor. A rough calculation of the maximum value of E_0 may be done as follows: $E_{0,\max} = \frac{1}{2} K(3\varepsilon_{rr})^2 V_m$ where K is the bulk modulus for the glass, ε_{rr} and V_m are the linear strain, and molar volume of glass respectively. ε_{rr} is approximately equal to

$$\left\{\frac{r_{K^+} - r_{Na^+}}{r_{K^+} + r_{SO_4^{2-}}}\right\}.$$

Since, Na^+ can be looked upon as going into the K^+ sites. Using the appropriate value of radii, V_m and K ($\sim 10^{10}$ dynes/cm^2), this energy turns out to be 5 to 6 kcal which is not too high in view of assumptions involved.

The random close packing model, therefore, seems to account for a number of experimental observations. Hence it is appropriate to examine in its purview why the easy glass formation in these systems is confined to certain regions of

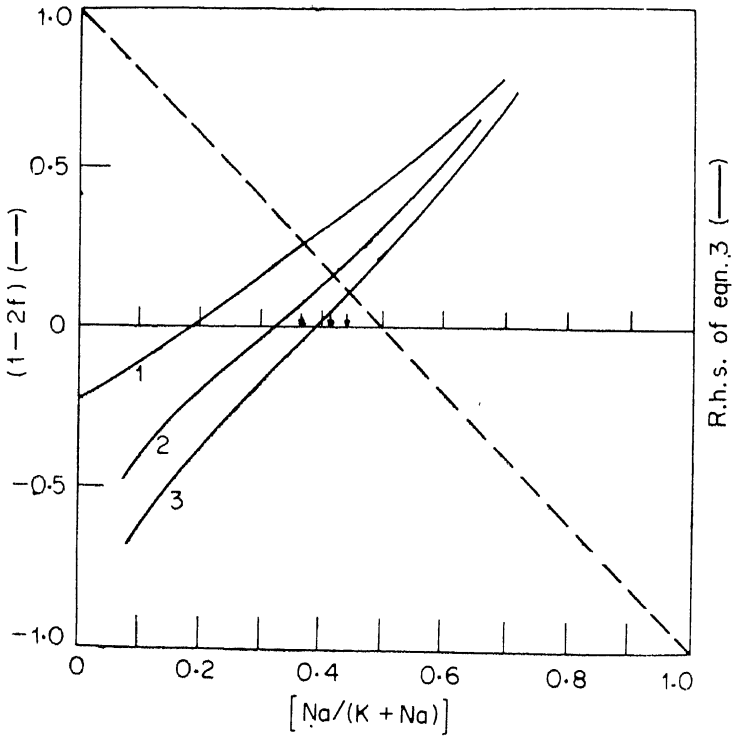

Figure 23. Graphical solution of the equation (see text) for finding f in the mixed-alkali effect. Curves (1), (2) and (3) correspond to x values of 0·7, 0·6 and 0·5. Evaluation was done with $\varepsilon_0 = 1$ kcal and $T = 415$ K. The solutions (f values) are indicated by arrows.

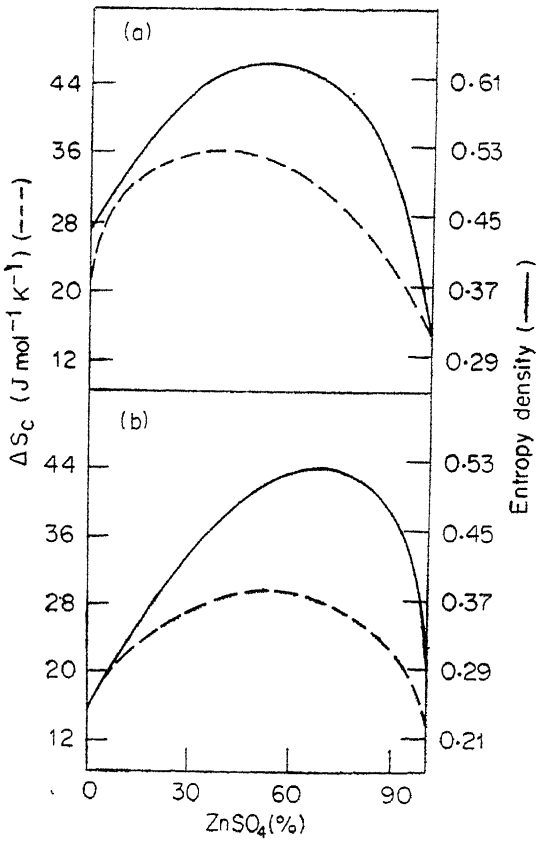

Figure 24. Variations of entropy and entropy densities in (a) ternary and (b) binary glasses.

composition, namely, 30–80 mole per cent of $ZnSO_4$. One feels intuitively that the ease of glass formation should be related to the configurational entropy of the glass forming system. On a heuristic basis the configurational entropies and entropy densities of the various binary and ternary glasses have been plotted as a function of composition as shown in figure 24. The entropies are approximate and evaluated on the basis of the random close packing model, giving importance to the variety of cation oxygen contacts which enhance the entropies of the systems. It appears that ease of glass formation is confined to regions of high entropies.

It is thus possible to account for most of the experimental observations by making use of a random close-packing assumption. It is interesting to note that a micro-crystalline approach is unnecessary for ionic glasses of this type, though the presence of strong coulombic interactions might at first sight make it appear that the micro crystalline model is more appropriate.

Acknowledgements

Thanks are due to Professor C N R Rao for his encouragement, Mr P S L Narasimham and Mr H G K Sundar have collaborated on various aspects of the

work presented here. Thanks are due to the Department of Science and Technology for financial help.

References

Angell C A and Helphrey D 1971 *J. Phys. Chem.* 7523
Bates 1960 in *Modern aspects of vitreons states* ed J D Mackenzie (London : Butterworths) 3
Bernal J D 1965 *Liquids, structures, properties, solid interactions* ed T T Hughel (Amsterdam : Elsevier)
Cargill G S 1975 *Solid state physics* eds H Ehrenreich, F Seitz and D Tunbull (New York : Academic Press) 30 227
Gattow G and Zemann J 1958 *Z. Anorg. Allg. Chem.* **293** 233
Glass A M, Lines M E, Nassan K and Shierer J W 1977 *Appl. Phys. Lett.* **31** 249
Johari G P and Goldstein M 1970 *J. Chem. Phys.* **53** 2372
Miller P J 1979 *J. Chem. Phys.* **71** 997
Narasimham P S L and Rao K J 1978a *J. Non-Cryst. Solids* **27** 225
Narasimham P S L and Rao K J 1978b *Proc Indian Acad. Sci.* (*Chem. Sci.*) **A87** 275
Narasimham P S L and Rao K J 1979a *Bull. Mater. Sci.* **1** 71
Narasimham P S L, Mahadevan S and Rao K J 1979b *Proc. Indian Acad. Sci.* (*Chem. Sci.*) **A88** 11
Polk D E 1970 *Scripta Met.* **4** 117
Polk D E 1972 *Acta Metall.* **20** 485
Rao K J, Helphrey D and Angell C A 1973 *Phys. Chem. Glasses* **14** 26
Rao K J and Sundar H G K 1980 *Phys. Chem. Glasses* **21** 216
Sunder H G K and Rao K J 1980 *J. Chem. Soc. Faraday Trans. I Chem.* **76** 1617
Yamane M and Mackenzie J D 1974 *J. Non-Cryst. Solids* **15** 153